A Performance Characteristic for Net Light Collection in Hyperspectral and Conventional Cameras: A^*

Torbjørn Skauli, *Member, IEEE*

***Abstract*— The signal-to-noise ratio of modern cameras under normal operating conditions tends to be limited by "photon noise" originating from the random arrival of photons. For best signal-to-noise ratio, it is desirable to collect as much light as possible, and to avoid losses internally in the camera. There is currently no widely accepted metric for the resulting net light collection, which depends on many aspects of camera design. The IEEE Standards Association P4001 group is developing a standard for hyperspectral imaging, including ways to fully specify camera performance in an efficient way. Motivated by P4001 requirements, this work proposes to specify the net light collection in a single quantity, denoted A^*, essentially defined as the product of nominal geometrical étendue, optics transmission, and detector quantum efficiency. It is shown how A^* can be physically interpreted as the detector pixel area of an equivalent lossless camera whose exit pupil subtends 1 sr. This article discusses how this quantity can be used as a figure of merit applying to hyperspectral cameras as well as to conventional multispectral and broadband cameras and other sensing systems employing imaging optics.**

***Index Terms*— Camera, étendue, F-number, hyperspectral, imaging, photography, specification, spectroscopy, standard, T-number, throughput.**

I. Introduction

CAMERAS of various types are widely used in remote sensing applications, where there are often stringent requirements on performance and calibration. Specification of cameras is therefore of particular importance in the remote sensing field. This is not least true for hyperspectral imaging, where the quality of image processing products depends on the integrity of spectroradiometric measurements of incoming light in each pixel. It turns out, however, that the state of the art of specifying commercial hyperspectral cameras currently falls short of what is needed to convey the actual performance to users and potential buyers [1]. Motivated in part by this situation, the IEEE Standards Association has established Project 4001 "Standard for Characterization and Calibration of Ultraviolet Through Shortwave Infrared (250 to 2500 nm) Hyperspectral Imaging Devices" [2] (P4001), sponsored by the IEEE Geoscience and Remote Sensing Society standards committee. A central task for P4001 is to define a set of performance characteristics which express camera performance in a complete but nonredundant way. The P4001 standard will consider the camera as a "black box," and define characteristics that are independent of the camera internals as far as possible, in order to be applicable to a range of current and possible future camera architectures.

Noise is a limitation on the quality of images and derived information products. In digital cameras today, the dominating noise is normally due to the random arrival of photons. As outlined in Section II-A, the signal-to-noise ratio depends on the amount of light collected by the camera. There is a well-established formalism for modeling camera light collection in terms of the properties of optics and detector separately [3]. With the camera considered as a "black box," it is the combined effect of these camera internals that is observable externally as a net light collection determining the signal-to-noise ratio. Therefore, P4001 requires a single characteristic to represent this net light collection. Paradoxically, a suitable characteristic for overall net light collection is not part of current standardized or customary ways of characterizing a camera.

This article introduces a way to analyze the radiometric properties of a "black box" camera with a degree of mathematical rigor, to make explicit some assumptions that are not always clearly stated, and to develop the underpinnings of a specification of light collection in P4001. A favored approach for expressing the net light collection is identified, which can be used as a parameter in a signal model, as an element of image metadata, and as a comparative figure of merit for camera light collection. This article elaborates on concepts discussed in conference papers [4], [5], [6], aiming to clarify issues and questions that can arise in the use of the proposed metric. The treatment applies not only to hyperspectral cameras but also to multispectral or broadband/monochrome cameras, as well as to other optical sensing systems employing imaging optics.

II. Brief Review of Related Work

A. Camera Signal Models

Conventional models for the signal from a camera, such as in [3, Sec. 7.3], are based on the detailed properties of internal camera components, such as imaging optics, spectrometer

Manuscript received 14 October 2022; revised 26 November 2022; accepted 4 December 2022. Date of publication 9 December 2022; date of current version 27 December 2022. This work was supported in part by the Research Council of Norway through the Center for Space Sensors and Systems, under Grant 309835.

The author is with the Department of Technology Systems, University of Oslo, 2007 Kjeller, Norway, and also with the Norwegian Defense Research Establishment (FFI), 2007 Kjeller, Norway (e-mail: torbjorn.skauli@its.uio.no).

Digital Object Identifier 10.1109/TGRS.2022.3228071

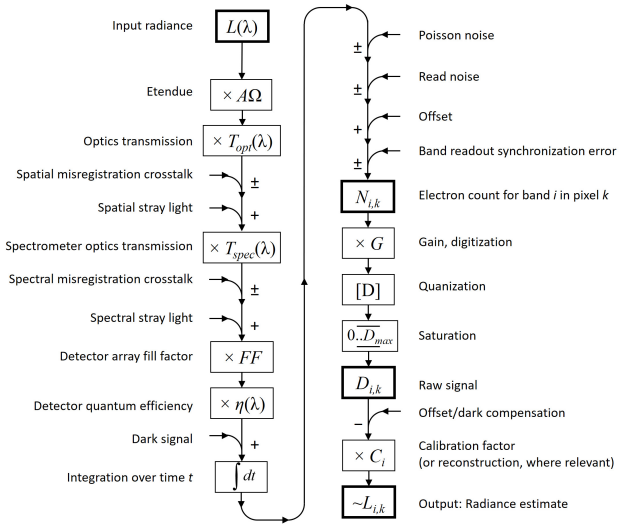

Fig. 1. Notional illustration of the signal chain in a camera (see text). Boxes with bold outlines indicate the main signal stages.

optics, and detectors. Many textbook treatments establish signal models which also include factors external to the camera, such as illuminants or atmosphere. Here, only the camera will be considered, in keeping with the needs of P4001.

With few exceptions (notably uncooled thermal cameras), modern cameras employ image sensors (also called focal plane arrays), where the individual elements are photon detectors (also called quantum detectors). In such detectors, the initial electronic signal is a count N_e of photoelectrons, excited by incoming photons. Most cameras do not count single electrons, but instead measure their total charge as an analog value, which is digitized to become the raw image data. These data, often called "digital numbers" (DN), are essentially proportional to N_e, but scaled by analog gain and digitization.

The photoelectron signal exhibits noise due to the random arrival of photons, often referred to as "photon noise." This noise follows a Poisson distribution, such that the variance is equal to the mean. An important point is that photon noise is the dominating noise contribution under normal operation of most modern cameras. The signal-to-noise ratio can then be estimated from

$$\mathrm{SNR} = \frac{N_e}{\sqrt{\mathrm{Var}(N_e)}} = \frac{N_e}{\sqrt{N_e}} = \sqrt{N_e}. \tag{1}$$

Strictly, this equation is exact only when N_e is equal to its expectation value, but except for very low signal levels, the noise can be estimated to good accuracy from the actual sampled N_e. It can be noted that such noise estimates may have been underutilized in image processing and exploitation [7]. An important aspect of the treatment here is to simplify estimation of this signal-dependent noise from image data.

Fig. 1 illustrates schematically the signal chain for a hyperspectral camera, from the incoming radiance level to an output radiance estimate. Nominally, a single data sample at the output represents light collected within a certain solid angle Ω and area A, whose product $A\Omega$ is known as the étendue. In reality, losses occur due to imperfect transmission in the imaging optics ($T_{\mathrm{opt}} < 1$) and the spectrometer optics ($T_{\mathrm{spect}} < 1$). Losses also occur in the detector itself due to nonideal quantum efficiency (QE) ($\eta_{\mathrm{det}} < 1$) and fill factor ($FF < 1$). Generally, the losses depend on wavelength λ (often strongly so, such as near the detector cut-off wavelength).

The optical signal can be distorted by coregistration errors or by stray light, and beyond about 2 μm wavelength also by thermally emitted radiation inside the camera. In the detector and electronics, the electrical signal can be distorted by dark current, offsets, or timing errors. Some of these distortions tend to act as a constant offset, and can be measured by momentarily blocking the light input, often with a shutter built into the camera. The treatment here will assume that such offsets are measured and compensated for in the output data. Other distortions, such as those due to coregistration errors or stray light, will depend on the incoming light, or on the camera operating conditions, and cannot be easily corrected for. Here, these distortions are neglected, but the P4001 standard will include ways to specify such effects.

A lower limit on the total noise is set by the readout noise generated in the detector and readout electronics. Here, for simplicity, readout noise is taken to include also noise from dark current (including contributions from any internally emitted light), and the dependence of this noise on integration time is ignored. The rms amplitude of this overall readout noise is represented as an equivalent electron count denoted σ_r, which also includes quantization noise from the digitization.

The signal may also be distorted by *saturation*, an upper limit on the signal range originating in the detector, in the analog electronics, or in the digitization. In the treatment here, saturation effects will be ignored for simplicity. The saturation level and readout noise together determine the dynamic range of the camera. For specification of dynamic range, the P4001 drafted method is as described in [4], which makes use of the concepts described in more detail here.

The signal model outlined in Fig. 1 can give a complete description of the radiometric behavior of the camera, for example for design purposes. However, such a model is more complex than what is needed to describe the overall "black box" performance of a camera in a specification, or to describe the properties of image data in accompanying metadata. For these purposes, which are main objectives of P4001, it is desirable to represent the camera by a minimal set of characteristics, essentially by performing a "parameter extraction" from the detailed model illustrated in Fig. 1. This article focuses on parameterization of the overall light collection for a single light sample, as one of several parameters in the P4001 signal model.

Noting that the photoelectron Poisson noise normally dominates, and also that the noise floor and saturation level can be conveniently expressed as equivalent photoelectron counts, it is clear that N_e is a desirable target for a camera signal model, even if the camera output normally is scaled to represent other quantities such as radiance, reflectance, or simply the raw DN. Fortunately, N_e can still be estimated from output data recorded in controlled conditions, as outlined in Section II-C. Therefore, this article will consider models for N_e, but the

results are still relevant for cameras where image data consist of radiance or reflectance values, or raw digital data.

B. Camera Characteristics Currently in Use

Conventional camera specifications today tend to have some heritage from the time when the recording medium was an exchangeable film. The specification of a camera was then essentially a specification of the lens. Traditionally, light collection by a lens is specified in terms of the F-number, the ratio of focal length to entrance pupil diameter. An alternative quantity is the numerical aperture, which expresses the same geometrical relation via the opening angle of the focused light cone on the image side of the lens. More information is contained in the T-number, which incorporates the effect of lens transmission and expresses the net light collection as an equivalent F-number of a lossless lens. The transmission is sometimes also given as a separate lens characteristic.

The widely used International Organization for Standardization (ISO) sensitivity rating, defined in ISO12233 [8], characterizes the sensitivity of a camera in terms of the amount of visible light needed at the image sensor (or film) to record an image whose noise level is negligible for visual viewing. Taken together with the F-number of the lens, the ISO rating is a fairly robust measure of light collection in photographic cameras. However, the ISO rating is specific to visible-light photography and does not generalize readily to other wavelength ranges or to machine vision applications.

A number of characteristics are in use for specifying light collection by the image sensor. The pixel pitch gives the nominal light collection area for a single light sample. Together with the wavelength-dependent QE, this gives fairly complete information about light collection at the image sensor. In some cases, a fill factor must be considered to account for the fraction of area on the image sensor that is actually sensitive to light. Detector sensitivity is also often specified in terms of detector noise, for example specified as readout noise in electrons, or as a normalized detectivity D^* [9]. However, these noise characteristics are less important in normal operating conditions where the dominating noise comes from the incoming photon stream. The European Machine Vision Association 1288 (EMVA1288) standard [10] defines a comprehensive way to specify many physical characteristics of an image sensor and its associated drive electronics.

Nowadays, in applications ranging from mobile phones to satellites, digital cameras are integrated units containing an image sensor and optics. This motivates the P4001 "black box" approach to camera specification, and more generally, it also suggests a reconsideration of how cameras are specified. Complete cameras are often specified giving both F-number and pixel pitch. This enables estimation of a nominal étendue, which can be used as a rough comparative measure of light collection. However, information about optics transmission and detector quantum efficiency is often missing. Sometimes, the camera is described by a "radiometric coefficient," a ratio between some form of output value, such as DN, and the input radiance. See for example [11]. However, there is no specific definition of the radiometric coefficient. Also, its value will depend on a variety of factors, such as electronic gain, that have no first-order impact on camera performance. The radiometric coefficient is therefore not a suitable figure of merit for the net light collection in a camera.

From the point of view of P4001, existing metrics for light collection are not well suited as comparative figures of merit for the performance of a hyperspectral camera. This situation has motivated the work presented here.

C. Measuring Photoelectron Count by "Photon Transfer"

Consider a case where the camera output data, denoted S, represent photoelectron counts scaled by some unknown gain factor G_S, for example to raw DN values or to radiance estimates. It is possible to use the "photon transfer" technique [12], outlined here, to retrieve the photoelectron count N_e. By making repeated measurements of the output value S at a constant input light level, the observed mean signal is related to the mean photoelectron count as

$$\overline{S} = G_S \overline{N}_e. \tag{2}$$

Also directly observable is the variance or the standard deviation of S which, knowing that N_e is Poisson distributed, can be written

$$\mathrm{Var}(S) = \mathrm{SD}(S)^2 = G_S^2\left[\mathrm{Var}(N_e) + \sigma_r^2\right] = G_S^2\left(\overline{N}_e + \sigma_r^2\right) \tag{3}$$

where σ_r is the readout noise amplitude. The signal-to-noise ratio is then

$$\mathrm{SNR} = \frac{\overline{S}}{\mathrm{SD}(S)} = \frac{\overline{N}_e}{\sqrt{\overline{N}_e + \sigma_r^2}}. \tag{4}$$

Under normal operation of a camera, the signal level tends to be sufficiently high that photon noise dominates, and readout noise is negligible. Then, the scaling factor G_S is simply determinable from (2) and (3)

$$\frac{\mathrm{Var}(S)}{\overline{S}} = \frac{G_S^2 \overline{N}_e}{G_S \overline{N}_e} = G_S. \tag{5}$$

With this estimate of G_S, the electron count corresponding to an output value S can be found from $N_e = S/G_S$. The photoelectron count N_e can therefore be considered an observable quantity for a "black box" camera.

A full photon transfer analysis can also determine the readout noise, dark current, and saturation level [12].

III. Signal Model for a "Black Box" Camera

A. General Model of Camera Response

This section introduces a mathematical description of the signal from a "black box" camera, without reference to internal parts. Consider for simplicity a camera viewing a scene at optical infinity, illustrated in Fig. 2. The input is then a distribution of light over wavelength λ and over the spherical coordinates θ, ϕ for angle of arrival of light, as well as over the position of arrival x, y in the entrance pupil plane, and over the time of arrival t. This input can be represented by a photon spectral radiance[1] $L_{\lambda q}(\lambda, \theta, \phi, x, y, t)$ with dimension

[1]The subscript λ is used to denote a spectral distribution ("per wavelength"), and the subscript q indicates quantum/photon units (as opposed to energy units).

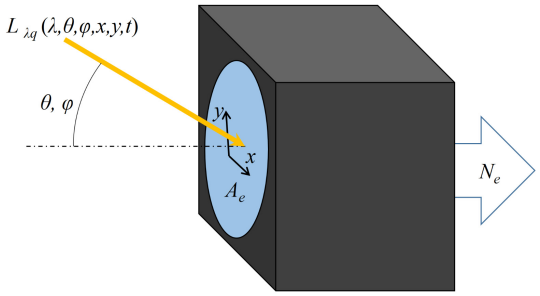

Fig. 2. "Black box" camera model. The camera receives a spectral photon radiance; a distribution of light over time, wavelength, and angles of arrival, as well as over position in the entrance aperture area. Output signals are taken to be electron counts N_e, since this quantity can be retrieved from other types of output by a "photon transfer" analysis.

$[L_{\lambda q}] =$ photons/(time $\times$ area $\times$ solid angle $\times$ wavelength). Note that assuming a scene at infinity represents no loss of generality. For a camera viewing an object at a finite distance, the angular coordinates θ and ϕ can be replaced by spatial coordinates in the object plane.

A single sampling of a light level, in the form of a photoelectron count $N_{e,ij}$ from a single detector element, is here taken to represent the amount of light in a given pixel i in a band j in the output image, recorded within a given integration time t_{int}. This neglects for now the possibility of binning or resampling as part of the signal chain, which is discussed later. The spectral, angular, spatial, and temporal selection of light by the camera (not only the detector) can be expressed as an overall QE $\eta_{\text{cam},ij}(\lambda,\theta,\phi,x,y,t)$ for band j in pixel i. This quantity is the probability that a photon with a given wavelength, arriving from a given angle at a given position in the camera entrance pupil at a time t, will give rise to a photoelectron in the signal for pixel i and band j. In other words, $\eta_{\text{cam},ij}$ describes image sharpness, spectral selection, transmission losses, etc. It is a sharply peaked function in the angular coordinates, centered on the direction corresponding to pixel i, and will be nonzero only within a given integration time t_{int} and within the entrance pupil in the (x, y) plane. For a hyperspectral camera, the wavelength dependence of $\eta_{cam,ij}$ will also be sharply peaked, with the peak located at the center wavelength of band j. Mathematically, $\eta_{\text{cam},ij}$ is dimensionless, but notionally it has dimension $[\eta_{\text{cam},ij}] =$ electrons/photon.

The expectation value of the photoelectron signal can then be written

$$N_{e,ij} = \int_{\lambda}\iint_{\Omega}\iint_{A}\int_{t}\eta_{\text{cam},ij}(\lambda,\theta,\phi,x,y,t) \times L_{\lambda q}(\lambda,\theta,\phi,x,y,t)\,\mathrm{d}t\,\mathrm{d}A\,\mathrm{d}\Omega\,\mathrm{d}\lambda \tag{6}$$

where the integrals over solid angle Ω and area A run over the hemisphere in front of the camera and over an infinite (in principle) plane containing the entrance pupil, respectively. Similarly, the integrals over λ and t run over all wavelengths and over all time. In this basic camera signal model, $\eta_{\text{cam},ij}$ thus represents the selection of incoming light by the camera in many dimensions. Starting the analysis at this general form, and transforming to a more conventional camera model in the following, will make underlying assumptions explicit.

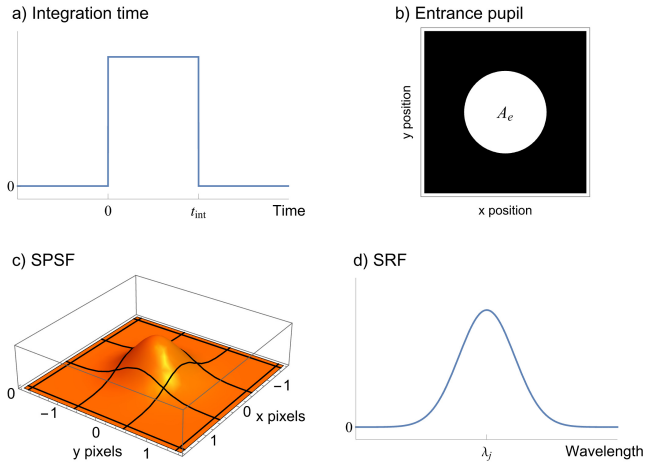

Fig. 3. Illustration of response functions for the light collection of a camera over many dimensions for a sampled light value in the image: (a) Collection over integration time t_{int}. (b) Collection within the entrance pupil area A_e of the camera. (c) Distribution of light collection over the angular coordinates of the scene, as described by the SPSF for a given center pixel. (d) Distribution of light collection over wavelength, as described by the SRF for a given band. See text.

B. Light Collection Over Time and Over Pupil Area

In the temporal dimension, the camera records an integral of the incoming light signal over some integration time t_{int}. The speed and precision of image sensor electronics are such that for most common camera applications, it is a good approximation[2] to assume a well-defined abrupt start and end of the integration, as illustrated in Fig. 3(a). Since only the integral is observed, not the instantaneous value, the signal model can be formulated assuming that the light level is constant in time and equal to its mean value over t_{int}. The integral over time in (6) then reduces to a multiplication by t_{int}.

A similar argument can be applied for light collection over the entrance pupil plane (x, y). The observed light level is an average over the entrance pupil area A_e. In many cases, such as in remote sensing, the camera is receiving light from a source with no strong directivity, located far away relative to the entrance pupil size, such as a sunlit landscape. It is then a good approximation to assume that the incoming light level is constant across the entrance pupil. A calibration source will normally also provide such uniform illumination. A further, often tacit assumption is that the camera response is uniform across the entrance pupil. Even in cases where this assumption does not hold well, the camera QE can be taken as a constant average response across the entrance pupil area as long as the light level tends to be uniform in the pupil plane. The signal model can then be formulated assuming that a uniform light level illuminates an entrance pupil plane with uniform response and with area A_e, as illustrated in Fig. 3(b). The integration over the entrance pupil plane in (6) then reduces to a multiplication by A_e.

[2]This neglects residual effects such as rise/fall times, timing jitter, "image lag," and "shutter efficiency."

With these simplifying assumptions, the signal model becomes

$$N_{e,ij} = t_{\text{int}} A_e \int_\lambda \iint_\Omega \eta_{\text{cam},ij}(\lambda,\theta,\phi) L_{\lambda q}(\lambda,\theta,\phi)\,\mathrm{d}\Omega\,\mathrm{d}\lambda \quad (7)$$

where $\eta_{\text{cam},ij}(\lambda,\theta,\phi)$ denotes the average of $\eta_{\text{cam},ij}(\lambda,\theta,\phi,x,y,t)$ over the integration time and over the entrance pupil area. Similarly, $L_{\lambda q}(\lambda,\theta,\phi)$ is the input light averaged over the integration time and entrance pupil. This is of course an often-used simplification for expressing the input to a camera.

C. Spectral and Spatial Response Functions

Now consider the selection of light by the camera over wavelength and angle of arrival, described by $\eta_{\text{cam},ij}(\lambda,\theta,\phi)$. The spectral and angular resolution can be described by what can be termed the spectral–spatial sampling function (SSSF)

$$\text{SSSF}_{ij}(\lambda,\theta,\phi) = \tfrac{1}{C}\eta_{\text{cam},ij}(\lambda,\theta,\phi) \quad (8)$$

where the normalization factor

$$C = \int_\lambda \iint_\Omega \eta_{\text{cam},ij}(\lambda,\theta,\phi)\,\mathrm{d}\Omega\,\mathrm{d}\lambda \quad (9)$$

has physical dimension [C] = (wavelength × solid angle). The SSSF is a distribution function representing the variation of camera response over wavelength and angle of arrival. ([13] uses the term "3-D PSF.") It has physical dimension [SSSF] = (wavelength × solid angle)$^{-1}$, and unit integral

$$\int_\lambda \iint_\Omega \text{SSSF}_{ij}(\lambda,\theta,\phi)\,\mathrm{d}\Omega\,\mathrm{d}\lambda = 1. \quad (10)$$

Angular resolution[3] is determined by the angular distribution of sensitivity expressed by $\text{SSSF}_{ij}(\lambda,\theta,\phi)$, determined for a large part by the point spread function (PSF) of the optics, but also by the detector element size, and in some cases by optical elements such as a slit. The angular distribution of sensitivity in the scene for the sampling of radiance in a pixel can be termed the *sampling point spread function* (SPSF), defined as

$$\text{SPSF}_{ij}(\theta,\phi) = \int_0^\infty \text{SSSF}_{ij}(\lambda,\theta,\phi)\,\mathrm{d}\lambda \quad (11)$$

for pixel i and band j. From (10), the SPSF has unit integral, and its physical dimension is [SPSF] = (solid angle)$^{-1}$. The SPSF contains full information about the angular resolution for the given band and pixel.

Similarly, the distribution of response over wavelength, the *spectral response function* (SRF), can be found by integrating the response over all directions of arrival

$$\text{SRF}_{ij}(\lambda) = \iint_\Omega \text{SSSF}_{ij}(\lambda,\theta,\phi)\,\mathrm{d}\Omega. \quad (12)$$

The SRF also has unit integral, and its physical dimension is [SRF] = (wavelength)$^{-1}$. For a conventional camera, the SRF contains information about the spectral response. For a hyperspectral camera, the set of SRFs for all bands contains information about the spectral resolution. The SPSF and SRF are illustrated in Fig. 3.

It is convenient to assume that the SSSF is separable:

$$\text{SSSF}_{ij}(\lambda,\theta,\phi) \approx \text{SRF}_{ij}(\lambda)\text{SPSF}_{ij}(\theta,\phi). \quad (13)$$

This is normally a good approximation and, in fact, an assumption which is rarely made explicit,[4] as pointed out in [13], but some discussion is given in for example [3], [14] and [15]. The signal model can now be written in terms of the SRF and SPSF using (9)

$$N_{e,ij} = t_{\text{int}} A_e C \int_\lambda \iint_\Omega \text{SRF}_{ij}(\lambda)\text{SPSF}_{ij}(\theta,\phi) \times L_{\lambda q}(\lambda,\theta,\phi)\,\mathrm{d}\Omega\,\mathrm{d}\lambda. \quad (14)$$

In some cases, such as when the camera is viewing a uniform broadband calibration source, the incoming photon radiance varies smoothly and slowly over angle of arrival and over wavelength. The input radiance can then be taken to have a constant value $L_{\lambda q,ij}$, at least locally around the pixel i and band j under consideration. This constant radiance can be taken as a multiplicative prefactor in (14), and the integral evaluates to 1. The signal model (14) for uniform radiance then becomes

$$N_{e,ij} = t_{\text{int}} A_e C L_{\lambda q,ij}. \quad (15)$$

Here, the product $A_e C$ is an overall radiometric coefficient for the camera.

D. Signal Model for Monochromatic Light in a Single-Band Camera

Now consider, for a while, the simpler case of a monochrome camera with some spectral distribution of sensitivity (which can of course represent a single band in a hyperspectral camera). Consider first the case where the incoming light is monochromatic with wavelength λ, and uniform in an angular region around pixel i, with an incoming photon radiance[5] $L_{q,i}$. For this single-band case, the band index j is dropped, and an explicit wavelength dependence is included instead. For a pixel i in the monochromatic case, (7) becomes

$$N_{e,i} = t_{\text{int}} A_e L_{q,i} \iint_\Omega \eta_{\text{cam},i}(\lambda,\theta,\phi)\,\mathrm{d}\Omega. \quad (16)$$

Here, the integral over $\eta_{\text{cam},i}$ is a constant with physical dimension of solid angle, expressing angular light collection, as well as losses in the camera, for this particular pixel. Note that the signal model (16) can be established by external measurements on the black box camera in Fig. 2. The radiance at the camera can be measured, the entrance pupil can be observed (by looking into the camera, or by a spot scan), the integration time is assumed to be accurately settable, and the electron count can be observed via photon transfer analysis. Then, the integral $\iint \eta_{\text{cam},i}(\lambda,\theta,\phi)\,\mathrm{d}\Omega$ is the only

[3]The term "spatial resolution" would often be used, but as illustrated in Fig. 2, positions in a scene at optically infinite distance are strictly directions described by polar angles. Therefore, "angular resolution" is used here, to avoid confusion with spatial coordinates in the entrance aperture plane.

[4]It can be noted that it has already been assumed in (7) that the dependences of $\eta_{cam,ij}(\lambda,\theta,\phi,x,y,t)$ on time t and position (x,y) are separable, by taking A_e and t_{int} as simple multiplicative factors. Strictly, some concepts for spectral imaging do violate these assumptions, for example multiaperture cameras, or cameras based on tunable filters.

[5]With dimension $[L_{\lambda,ph}]$ = photons / (time × area × solid angle).

unknown quantity, and can be considered as an experimentally determined calibration factor.

Since the integral in (16) accounts for both losses and angular light collection, it would be preferable to represent it as a product of these two effects, defined as

$$\Delta\Omega_i \eta_i(\lambda) \equiv \iint_{\Omega} \eta_{\mathrm{cam},i}(\lambda, \theta, \phi)\, \mathrm{d}\Omega. \tag{17}$$

Here, $\Delta\Omega_i$ is an equivalent instantaneous field of view (IFOV) for pixel i, and $\eta_i(\lambda)$ is a factor in the range $0, \ldots, 1$ accounting for light loss at the given wavelength for this pixel. The signal model for monochromatic light will then simplify to

$$N_{e,i} = t_{\mathrm{int}} A_e \Delta\Omega_i \eta_i(\lambda) L_{q,i}. \tag{18}$$

Here, we recognize the product $A_e \Delta\Omega_i$ as the étendue, or throughput, of the camera optics.

An issue with the form (18) is that given the observables listed earlier, it is not possible to determine the factors $\Delta\Omega_i$ and $\eta_i(\lambda)$ independently of each other. It can be argued that $\Delta\Omega_i$ represents the width of the SPSF, but there is no unique way to determine the size of the blur spot represented by the SPSF. However, for a "black box" camera, it is still possible to observe the pixel sampling interval in the scene. Then, it is reasonable to define $\Delta\Omega_i$ as the solid angle of the region of the field of view (FOV) bounded by lines drawn midway between pixel centers. Thus, if the angular sampling interval for pixels in the neighborhood of pixel i is found to be $\Delta\theta_i$ along the rows and columns of pixels then, since a pixel will have a small angular FOV, we have

$$\Delta\Omega_i = \Delta\theta_i^2. \tag{19}$$

Of course, it is possible for the sampling intervals to be different in the two spatial directions, defining a rectangular pixel region. Then, $\Delta\Omega_i$ will be the product of these intervals. This tends to be the case for the commonly used "imaging spectrometer" cameras operating in "pushbroom" scanning mode, where the pixel sampling interval is only observable in the direction along the slit (i.e., across the scan direction). The appropriate angle for light collection along the scan direction can then be taken to be the projection of the slit into the scene, which multiplied by the across-track sampling interval $\Delta\theta_i$ gives $\Delta\Omega_i$. This represents a minor deviation from the "black box" principle, since the slit width is not uniquely determinable from measurements outside the camera. (Except for cameras with exchangeable objective lenses, where the slit can be directly observed after removing the lens.) A similar issue arises for hyperspectral cameras based on a raster/whiskbroom scanned spectrometer, where $\Delta\Omega_i$ is defined by the projection of the aperture in the focal plane of the imaging optics through which light is fed to the spectrometer.

Thus, all the quantities in (18) can be considered as independently observable except $\eta_i(\lambda)$, which becomes an experimentally determined calibration factor. From (17), we find

$$\eta_i(\lambda) = \frac{1}{\Delta\Omega_i} \iint_{\Omega} \eta_{\mathrm{cam},i}(\lambda, \theta, \phi)\, \mathrm{d}\Omega = \frac{t_{\mathrm{int}} A_e L_{q,i}}{\Delta\Omega_i N_{e,i}}. \tag{20}$$

With this, the parameters in the signal model (18) can be determined from external observables. The model can then be used to predict the photoelectron count for a given light input, and thereby also the corresponding noise and signal-to-noise ratio.

Note that $\Delta\Omega_i$ as defined in (19) includes any insensitive area within the pixel on the image sensor, which can be specified in terms of a fill factor FF less than unity. In the treatment here, if the fill factor deviates from unity, it will be included in $\eta_i(\lambda)$, along with losses due to the optics transmission $T_{\mathrm{opt},i}(\lambda)$. For hyperspectral cameras, an additional factor is the spectrograph efficiency $T_{\mathrm{spec},j}(\lambda)$ for the wavelength-selective part of the optics. Obviously, the detector QE $\eta_{\mathrm{det}}(\lambda)$ is also a factor in $\eta_i(\lambda)$, which can then be notionally expressed as

$$\eta_i(\lambda) = T_{\mathrm{opt},i}(\lambda) \mathrm{T}_{\mathrm{spec}}(\lambda) FF\, \eta_{\mathrm{det}}(\lambda). \tag{21}$$

Thus, $\eta_i(\lambda)$ is a product containing all the different loss factors affecting the net light collection.

Conventional modeling of camera signals normally includes all the factors of (21) explicitly in (18), giving

$$N_{e,i} = t_{\mathrm{int}} A_e \Delta\Omega_i T_{opt,i}(\lambda) \mathrm{T}_{\mathrm{spec}}(\lambda) FF\, \eta_{det}(\lambda) L_{q,i}. \tag{22}$$

This expression illustrates the potential for simplifying signal models, and the need to do so in order to conform to the "black box" approach of P4001.

IV. Metric for Overall Light Collection: A^*

A. Definition of A^*

Real cameras span a wide range of values for all the factors in (22). Since these are multiplicative factors, only their product needs to be specified when a camera is characterized as a "black box." In practice, the camera user will often have an interest in setting or knowing t_{int}. The pixel IFOV $\Delta\Omega_i$ is important for the spatial interpretation of the image, but normally not for radiometric characterization. The other individual factors in (22), namely A_e, $T_{\mathrm{opt},i}(\lambda)$, $\mathrm{T}_{\mathrm{spec}}(\lambda)$, FF, and $\eta_{\mathrm{det}}(\lambda)$, are uninteresting to the camera user across a wide range of applications. It therefore makes sense to represent the camera light collection, in a given pixel and for a given wavelength, as a single quantity, here denoted A^* and defined as

$$A_i^*(\lambda) \equiv A_e \Delta\Omega_i \eta_i(\lambda). \tag{23}$$

Written out more explicitly using (21), this becomes

$$A_i^*(\lambda) = A_e \Delta\Omega_i T_{\mathrm{opt},i}(\lambda) \mathrm{T}_{\mathrm{spec}}(\lambda) FF\, \eta_{\mathrm{det}}(\lambda). \tag{24}$$

Thus, A^* is simply a product of the geometrical factors representing light collection by the optics, and the factors representing the loss of light through the optics and detector (also including loss of photoelectrons, where relevant). The signal model for monochromatic light with photon radiance $L_{q,i}$ then reduces to

$$N_{e,i} = t_{\mathrm{int}} A_i^*(\lambda) L_{q,i}. \tag{25}$$

This shows how the quantity A^* can represent the net light collection by the camera in a compact way, compared to (22).

With respect to specification and testing of a camera as a "black box," consider the quantities in the signal model expressed in (25). The monochromatic input radiance $L_{q,i}$ can

be measured, and the integration time t_i can be accurately set,[6] while the electron count $N_{e,i}$ is determinable from a "photon transfer" measurement. Thus

$$A_i^*(\lambda) = \frac{N_{e,i}}{t_{\text{int}} L_{q,i}} \tag{26}$$

is experimentally determinable without knowledge of camera internals. Measuring the wavelength-dependent $A_i^*(\lambda)$ requires a monochromatic calibration source, similar to what is required for determination of the QE for a detector, or the SRF for a camera. In a hyperspectral camera, each band j will have a different $A_{ij}^*(\lambda)$, peaking at their respective band centers, as discussed later.

B. Physical Interpretation of A^*

The quantity A^* can be given a physical interpretation by a notional transformation of the camera: First, observe that the étendue, given by $A_e \Delta\Omega_i$, is an invariant quantity through the camera optics. At the image sensor, the étendue is the product of the area of the detector element A_{det} and the solid angle Ω_{det} subtended by the exit pupil of the optics.[7] Thus, we have $A_{\text{det}}\Omega_{\text{det}} = A_e \Delta\Omega_i$. The signal model (23) can then be written

$$N_{e,i} = t_{\text{int}} A_{\text{det}} \Omega_{\text{det}} \eta_i(\lambda) L_{q,i}. \tag{27}$$

Keep in mind that if the size of the entire camera is scaled, angles are unchanged so that the pixel IFOV, as well as the FOV, are unchanged, while the étendue scales with the aperture area. Now assume the following transformation of the camera, which in each step maintains its radiometric properties, ending up with the same IFOV.

1) First, let losses in the camera be eliminated, and instead scale the camera so that the detector element area is reduced to $A'_{\text{det},i} = A_{\text{det}} \eta_i(\lambda)$. Then, the signal model becomes $N_{e,i} = t_{\text{int}} A'_{\text{det},i} \Omega_{\text{det}} L_{q,i}$.
2) Then, let the exit pupil of the optics be circular and subtending a solid angle such that the étendue would change by a factor[8] $1\,\text{sr}/\Omega_{\text{det}}$. Change the image sensor pixel area by the inverse of this factor to maintain throughput. The image sensor now receives radiation within a solid angle of 1 sr (see notes later), and the sensor pixel area has a value equal to $A_i^*(\lambda)$, giving the signal model (25).
3) Then, maintaining Ω_{det} at its notional value of 1 sr and keeping the sensor pixel area constant, let the focal length and diameter of the optics be scaled by the same factor so that the pixel IFOV returns to its original value for the new detector area.
4) Let the electrical properties of the detector, such as noise, dark current, and saturation level, be unchanged.

This transformation leads to a radiometrically equivalent camera where Ω_{det} is fixed at a notional value of 1 steradian seen from the image sensor, and the light collection of the real camera is expressed as a detector area equal in value to $A_i^*(\lambda)$.

The following notes must be made about the transformation to an equivalent camera.

1) The 1-steradian aperture is in the upper range of lens apertures that are realized in practice, but the equivalent camera here is only a mathematical construct.
2) In step 2 given earlier, a circular aperture subtends 1 sr if its aperture diameter is $f/0.78$, where f is the focal length. However, for the normal case of a planar detector, and the implicit assumption of planar lens principal surfaces, projection cosines reduce the light collection. Then, the aperture would need to be $f/0.73$ to maintain throughput. Since the actual values are determined on the object side of the optics, the small-angle approximation suffices for determination of the pixel IFOV $\Delta\Omega_i$. The equivalent camera is only a construct for interpretation; therefore, these finer points are not important for the use of A^* to quantify net light collection.
3) Taking solid angle to be dimensionless, the physical dimension of A^* is an area. It is suggested to report A^* values in units of μm^2, keeping in mind the interpretation given here. However, in radiometric calculations, such as (25), A^* values must be taken as an area–solid angle product.
4) For most cameras, Ω_{det} is smaller than that of the equivalent camera, and A^* will have a value smaller than the actual pixel area, even in the absence of losses.
5) In optical systems employing optical immersion of the detector, A^* can account for the resulting increase in étendue (see footnote).

The notation A^* and the interpretation as an equivalent camera are modeled on the established D^* quality metric for detectors [9]. D^* is the signal-to-noise ratio obtained in a signal bandwidth of 1 Hz with a detector with equivalent quality having an area of $1\,\text{cm}^2$ and receiving an optical power of 1 watt. Similarly, A^* is referenced to $\Omega_{\text{det}} = 1$ sr. It is noted that A^* is also the name of a graph search algorithm, but confusion appears unlikely.

C. A^* as a Figure of Merit

The preceding sections have shown that A^* can be seen as a figure of merit for light collection in an imaging system, and can be interpreted as the detector pixel area of a radiometrically equivalent camera with no losses and with a standardized geometry on the image sensor side of the optics. Arguably, the definition of A^* follows naturally from consideration of light collection by a "black box" camera, as a parameter that can be extracted from either a conventional signal model such as (22), or the more general model introduced in (6). The wavelength-dependent quantity $A^*(\lambda)$ is suited for specifying the overall spectral sensitivity characteristic of a complete camera in a

[6] If needed, the integration time can also be measured, for example using a pulsed light source with a controllable delay.

[7] A_{det} will normally be the same for all pixels, while Ω_{det} may vary somewhat across the FOV due to projection geometry or other variations, and therefore depend on the pixel index. The notional equivalent camera developed here is considered ideal; hence, a pixel index is omitted for Ω_{det}. Instead, variations in light collection are incorporated in $\eta_i(\lambda)$ so that the values of A^* will reflect such nonuniformities in the real camera.

[8] In optical systems employing optical immersion of the detector in a medium with refractive index n_{det}, use a factor $1\,\text{sr}/(n_{\text{det}}^2\Omega_{\text{det}})$, and let the transformed camera have no immersion.

similar way as the QE is used to characterize detectors and image sensors.

The introduction of A^* above considered the simple case of a single pixel receiving monochromatic light. The full set of $A_i^*(\lambda)$ for all pixels i can represent the detailed spectral response, as well as any response nonuniformities across the FOV. The remainder of this article discusses how the A^* concept can be developed into a more practical figure of merit for different types of camera, including cameras with multiple bands. However, the treatment here does not discuss how an aggregated A^* shall be reported across all pixels, which may vary depending on context. For example, a camera datasheet might include values for the mean and/or minimum A^* across all pixels. It is also possible to report the total light collection of the camera as a sum of A^* over all pixels. P4001 will include guidance on how to report pixel-aggregated values. In the following treatment, only a single pixel is considered.

D. Dependence of A^* on Aperture, Focus, and Focal Length

The dependence of A^* on camera settings is important to consider. In cases where a camera has a variable aperture, it would be reasonable to specify A^* for the largest aperture setting. The user can then calculate the actual light collection for a reduced aperture setting from the nominal ratio for different aperture settings, as is well established in classical photography. For cameras with adjustable focus, the effective aperture will vary with focus setting. This effect will be minor when the object distance is large compared to the focal length. In other cases, focus setting may need to be considered for proper specification of A^*.

Several hyperspectral camera architectures, notably the imaging spectrometer, consist of an objective lens (often referred to as "foreoptics"), dispersive spectrometer optics, and an image sensor. Many cameras have exchangeable objective lenses, and thus can be operated with different focal lengths. It will then be strongly preferable to use lenses whose étendue is at least large enough to fill the étendue of the spectrograph, regardless of the focal length. (Similarly, it tends to be wasteful to choose an objective lens with significantly larger étendue.) Therefore, the étendue of a hyperspectral camera will in many cases tend to be set by the spectrometer optics, independently of the choice of objective lens. Then, A^* will tend to be invariant to the choice of focal length, except in the less common case where one lens has a much larger transmission loss than another. Thus, since it has no first-order dependence on focal length, A^* can serve as a useful figure of merit for fair comparison of hyperspectral cameras even when the cameras have different focal lengths and pixel sizes.

V. A^* for Broadband and Multispectral Cameras

A. A^* Simplifies the Signal Model for a Broadband Camera

Although the main motivation for this work has been specification of hyperspectral cameras, it is instructive to first consider the case of a "monochrome" camera with broad spectral response, at the same time illustrating the potential usefulness of the A^* quantity for such cases. When the incoming light is distributed over wavelength with a spectral photon radiance

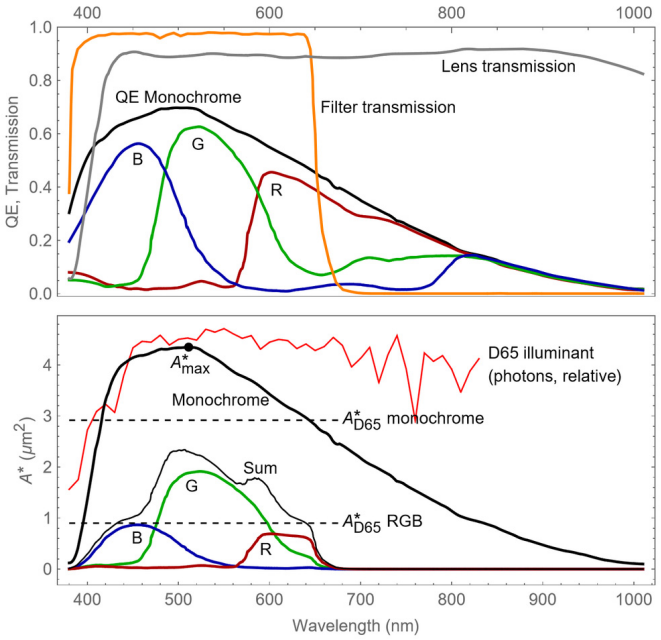

Fig. 4. Illustration of A^* for a monochrome camera and a multispectral (RGB color) camera based on example component data. Top: Specified QE for an image sensor (Sony IMX174) in monochrome and RGB color versions. Also shown are transmission spectra for a lens (Schneider Cinegon 1.9/10) and an IR cut filter (Schneider BP 515-270). Bottom: Graphs of A^* for monochrome and color cameras built from these components. The sum over all three color channels is also shown, as well as the relative photon spectrum of the CIE D65 illuminant. Overall values A^*_{D65} for this illuminant are shown by the dashed lines. Also shown is the peak value A^*_{max} for the monochrome case.

$L_{\lambda q}(\lambda)$, then the signal model (25) becomes an integral over wavelength with $A^*(\lambda)$ as a spectral weighting:

$$N_e = t_{\text{int}} \int_\lambda A^*(\lambda) L_{\lambda q}(\lambda) \mathrm{d}\lambda. \tag{28}$$

(Since only a single pixel is considered here, the pixel index is dropped for simplicity.) Thus, given a specified $A^*(\lambda)$, the photoelectron signal, and thereby the SNR, can be estimated for an arbitrary input spectrum in a simple way that eliminates the need to reference the camera internals in (24).

B. Calculating A^* From Component Properties

Values of A^* can be determined from component properties according to (24). Consider the example illustrated in Fig. 4 based on example data taken from commercial datasheets. The upper plot shows the wavelength-dependent QE of a complementary metal–oxide–semiconductor (CMOS) image sensor in monochrome and red-green-blue (RGB) versions. The plot also shows the transmission spectrum for a lens and an infrared (IR)-cut filter. In this example, the pixel pitch on the image sensor is 5.86 μm, and the lens focal length is 10 mm, giving an angular IFOV of 0.59 mrad and thus $\Delta\Omega_i = 0.34$ μsr. The lens F-number is 1.9 so that the entrance pupil is 5.2 mm in diameter, with an area of $A_e = 22$ mm^2, giving an étendue $A_e \Delta\Omega_i = 7.5$ μm^2. The lens and the monochrome image sensor make a camera with broad spectral response. A graph of the resulting $A^*(\lambda)$ is shown in the lower plot, peaking at 4.3 μm^2.

A three-band color camera can be made using the color version of the same image sensor, where color filters are

applied to individual detector pixels in a Bayer pattern. Groups of 2×2 pixels then have one red, two green, and one blue pixel, leading to average fill factors of 25%, 50%, and 25%, respectively, assuming a uniform source, and neglecting for simplicity the demosaicking operation. An "IR cut" filter must be added to block the near-IR (NIR) wavelengths not absorbed by the on-chip filters. It is evident from the lower plot in Fig. 4 that the light collection is drastically lower in the color camera, compared to the monochrome camera. The reduction is due a combination of light loss in the filters and the reduced fill factor inherent in the Bayer pattern. Comparing to the specified QE graphs for individual pixels on the image sensor, it is clear that the representation of overall light collection offered by A^* is informative about the relatively large differences between these two seemingly comparable cameras.

C. Predicting Signal-to-Noise Ratio From a Specified A^*

Starting from a specified A^*, signal levels can be estimated relatively easily. Consider imaging of a Lambertian white surface reflecting an $M_v = 100$ lux illumination, for simplicity taken to be at $\lambda = 555\,\text{nm}$ where the conversion factor $K = 683$ lumen per watt applies. The photon radiance input to the camera becomes

$$L_{ph} = \frac{\lambda}{hc}\frac{M_V}{\pi K} = 1.30 \times 10^{17}\ \text{photons}/m^2\text{sr}. \tag{29}$$

The A^* of the green channel of the color camera at 555 nm is $1.7\,\mu\text{m}^2$. Assuming video imaging with 30 ms integration time, (25) gives $N_e = 6570$ electrons, 20% of the specified saturation level. Readout noise is then negligible, and the signal-to-noise ratio is found from $\text{SNR} = (N_e)^{1/2} = 81$. Observe that the calculation of the signal level starting from a specified A^* is simplified by relieving the user from having to consider the separate factors in (21) and (25).

D. Defining an Overall A^* Value for a Camera

In some cases, it will be desirable to represent light collection performance for a camera by a single number. Taking the maximum value over all wavelengths A^*_{max} shown for the monochrome case in Fig. 4 may appear optimistic. However, this number could be seen as a fair indicator of the light collection capability at minimum loss, and thereby a figure of merit for the capability of the optical design. This quantity was proposed in an earlier work [6] together with a wavelength-dependent QE. This latter quantity is dropped in the treatment here, and A^* is instead defined as a wavelength-dependent quantity.

In many cases, a more conservative measure of light collection will be appropriate. Consider again the expression for A^* under monochromatic illumination in (26). If instead the illumination has some standardized broadband spectrum, it is still possible to obtain a corresponding value A^*_{std}, where the subscript can indicate the particular illuminant used (such as "A^*_{D65}" below). For a monochrome camera receiving a standard illuminant represented by a photon spectral radiance spectrum $L_{\lambda q,\text{std}}(\lambda)$, the signal model (28) can be written

$$N_e = t_{\text{int}} \int_\lambda A^*(\lambda) L_{\lambda q,\text{std}}(\lambda)\text{d}\lambda \equiv t_{\text{int}} A^*_{\text{std}} L_{q,\text{std}}. \tag{30}$$

This defines A^*_{std} as a characteristic for overall light collection for the standard illuminant spectrum, whose photon radiance integrated over all wavelengths is

$$L_{q,\text{std}} = \int_\lambda L_{\lambda q,\text{std}}(\lambda)\text{d}\lambda. \tag{31}$$

As an example, consider International Commission on Illumination (CIE) illuminant D65, shown in Fig. 4 as a relative photon spectral radiance. The overall value for this illuminant for the monochrome camera is $A^*_{D65} = 2.9\,\mu\text{m}^2$, as indicated by a dashed line in the figure.

In the case of a multispectral camera, light collection can be characterized according to (30) for each band. But it is also possible to define an overall value of A^* for the camera as the sum of A^* in all bands, illustrated in Fig. 4. For a standard illuminant $L_{\lambda q,\text{std}}(\lambda)$, the total signal in all bands then becomes a sum of the responses given by $A^*_j(\lambda)$ in each band j, integrated over wavelength as in (28)

$$N_e = t_{\text{int}} \int_\lambda \sum_j A^*_j(\lambda) L_{\lambda q,\text{std}}(\lambda)\text{d}\lambda \equiv t_{\text{int}} A^*_{\text{std}} L_{q,\text{std}}. \tag{32}$$

The overall A^* value defined in (31) and (32) can be found from the defined illuminant spectrum and the observed $A^*(\lambda)$ as

$$A^*_{\text{std}} = \frac{1}{L_{q,\text{std}}} \int_\lambda \sum_j A^*_j(\lambda) L_{\lambda q,\text{std}}(\lambda)\text{d}\lambda. \tag{33}$$

This is an overall value for A^* for all bands of a multispectral camera, weighted by the given illuminant spectrum. Note that this also incorporates the monochrome case in (30), for which the sum has only a single term. The range of integration is normally the range of wavelengths where both $L_{\lambda q,\text{std}}(\lambda)$ and $A^*(\lambda)$ are nonzero, but may need to be restricted to the range over which the standard illuminant is defined.

Clearly, A^*_{std} is a meaningful figure of merit for comparison of monochrome or multispectral cameras with respect to a given application where a representative illuminant spectrum can be defined. Notable examples would be color imaging under one of the CIE illuminants, as well as thermal imaging in an ambient temperature background.

In Fig. 4, dashed lines indicate the overall value for the CIE D65 illuminant, A^*_{D65}, for the monochrome ($2.9\,\mu\text{m}^2$) and color ($0.9\,\mu\text{m}^2$) camera configurations. With this metric, the color camera is found to have an effective light collection which is 31% of that of the monochrome camera. Of course, A^*_{D65} cannot alone account for the radiometric quality of a color camera. Since the definition of D65 extends into the tails of the eye response, it is at least also necessary to consider the color rendering of the camera. Nonetheless, assuming comparable color rendering, the quantity A^*_{D65}, or similar quantities for different CIE illuminants, can clearly be useful for comparing light collection between color cameras.

VI. A^* for Hyperspectral Cameras

A. Defining Per-Band A^*_j for Hyperspectral Cameras

In hyperspectral imaging, the bandwidths are small relative to the band center wavelength. It is then often reasonable

to assume that the spectral photon radiance is smooth and slowly varying within the band. In particular, this is a good approximation for the case of a hyperspectral camera viewing a calibration source based on thermal radiation from a tungsten lamp, as already discussed in relation to (15). This case is highly relevant for the P4001 standard. Here, only a single pixel is considered, thus the pixel index is dropped, and a single narrow band j is considered. Assume that the input is a calibration source whose photon spectral radiance $L_{\lambda q,\mathrm{cal}}(\lambda)$ is smooth relative to the bandwidth of the hyperspectral camera. The signal model can then be expressed as a product similar to (30), but with the bandwidth as an explicit factor $\Delta\lambda_j$:

$$N_{e,j} = t_{\mathrm{int}} \int_{\lambda} A_j^*(\lambda) L_{\lambda q,\mathrm{cal}}(\lambda) \mathrm{d}\lambda \equiv t_{\mathrm{int}} A_j^* \Delta\lambda_j L_{\lambda q,\mathrm{cal}}\left(\lambda_j\right). \tag{34}$$

In this notation, A_j^* is a single number representing light collection in band j centered at λ_j instead of a wavelength-dependent $A_j^*(\lambda)$ giving a detailed band profile as in (25). Also note that the input light is represented as a spectral photon radiance here, not a photon radiance as in (25). The bandwidth $\Delta\lambda_j$ must be determined from the shape of $A_j^*(\lambda)$ or by other means, as discussed in Section VI-B.

Equation (34) accounts well for cases where the incoming photon spectral radiance is approximately constant within the band, and also for cases where the spectral radiance varies linearly within the band and $A_j^*(\lambda)$ is symmetric. These conditions will tend to be well approximated by a hyperspectral camera viewing a calibration source. Then, given a suitable definition of bandwidth, values of A_j^* can be found from

$$A_j^* = \frac{N_{e,j}}{t_{\mathrm{int}} \Delta\lambda_j L_{\lambda q,\mathrm{cal}}\left(\lambda_j\right)} \tag{35}$$

for band j, based on observed $N_{e,j}$ for a known radiance input. Conversely, the incoming spectral radiance can be estimated from the signal value $N_{e,j}$ using A_j^* and $\Delta\lambda$. It can be noted that the resulting value of photon spectral radiance at the band center, $L_{\lambda q,\mathrm{cal}}(\lambda_j)$, may be inaccurate if the radiance spectrum is not smooth, or if $A_j^*(\lambda)$ has an irregular shape. This is of course a general limitation for a hyperspectral camera calibrated to produce spectral radiance values.

The usefulness of A^* for a hyperspectral camera arises in two ways. First, A_j^* values are of interest as metadata, since, together with the bandwidths, they allow the user to calculate the photoelectron count accurately (regardless of spectral shapes), and thereby estimate the signal-dependent SNR for each radiance value in an image cube. Second, since the bandwidth is taken as a separate factor in (34), the A_j^* values enable direct comparison between different hyperspectral cameras, for example represented as a graph of A_j^* over wavelength, even if their bandwidths differ. (Such a graph could look similar to the A^* graph for a monochrome camera in Fig. 4.) These two uses of A^* are currently drafted to be part of the P4001 standard.

B. Defining a Radiometric Bandwidth $\Delta\lambda_j$

In (34), differently from (26), measured values for $N_{e,j}$, t_{int} and $L_{\lambda q,j}$ are insufficient for unique determination of A_j^*. Only the product of A_j^* and $\Delta\lambda_j$ can be determined from the measurement, so that if the input spectrum is approximately constant around the band center, the effect of a change in $\Delta\lambda_j$ is indistinguishable from the same relative change in A_j^*. For the P4001 standard, this can reduce the informative value of these characteristics, and open up possibilities for artificial design adaptation to improve specified values of A_j^*. The fairness of the comparison of A^* between different cameras therefore hinges on the method used to define bandwidth for a given SRF. Even if the wavelength-dependent $A_j^*(\lambda)$ is measurable according to (26), and is normally sharply peaked around the band center wavelength λ_j, it is not straightforward to define a single quantity that represents the bandwidth $\Delta\lambda_j$ in a robust manner, as needed for the standard, considering measurement noise and the possibility of irregular peak shapes. An important practical consideration is that measurement of camera radiometric characteristics is significantly more convenient using a known broadband source (readily available) instead of a radiometrically calibrated tunable narrowband source (expensive, limited spectral range, limited stability, and/or limited radiance level).

Definition of peak width is a recurring issue in many fields (not to mention definition of "resolution"). In general, the definition of bandwidth can be based on: 1) parameters of a fit to a given functional form, such as a Gaussian; 2) a descriptive metric for the SRF such as the full width at half maximum (FWHM); or 3) the spectral sampling interval. In the field of spectroscopy, CIE233 [16] defines bandwidth as the width of a box-shaped SRF having the amplitude of the actual SRF at the band center. However, this approach is currently not part of the P4001 draft, because it would make the width dependent on the amplitude at a single point on the actual SRF, reducing robustness against irregular-shaped SRFs. Also, the band center position is not explicitly defined in CIE233.

The most common type of hyperspectral camera is based on a line imaging ("pushbroom") spectrometer architecture employing dispersive optics. Then, the light collection bandwidth is well defined by the maximum of projected slit width and detector width, scaled to a wavelength interval according to the camera dispersion [14]. The bandwidth then ideally corresponds to the width of the spectral bins illustrated in Fig. 5(a). This would be the spectral analog to the definition of spatial light collection in (19). The camera then performs an ideal averaging of the input spectrum within each band. In this case, both the bandwidth $\Delta\lambda_j$ and the band effective light collection A_j^* can be uniquely defined from the box-shaped SRF. However, this nominal bandwidth of a spectrometer will be unrealistically low, since the spectrometer optics inevitably will exhibit some degree of blur, leading to smearing of the actual spectral response as illustrated in (b). Observe that light lost from a given band signal due to blur is compensated by incoming light similarly lost from other bands. Therefore, the sum of light collection over all bands is still constant, as illustrated by the thick blue line. The sampling interval, equal to the nominal bin width, could then still be a reasonable estimate of bandwidth for radiometry purposes, even if the SRF peak is broadened.

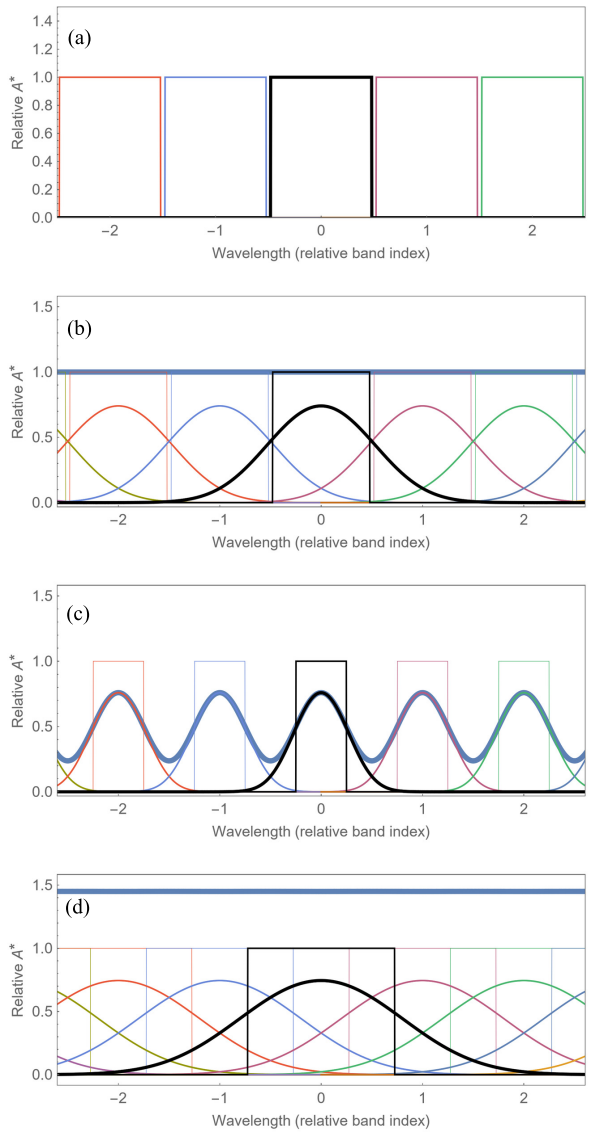

Fig. 5. Illustration of different cases of A^* wavelength dependence for a hyperspectral camera. (a) SRF for several bands in an ideal dispersive camera. (b) SRFs for a real dispersive camera with optical blur. The thick blue line shows the sum over all SPSFs. (c) Same as (b), but with a reduced detector fill factor. This can also represent a tunable filter with SRF peak width smaller than the spectral sampling interval. (d) Tunable filter camera with overlapping bands. Thin lines illustrate notional box-shaped SPSFs overlapping.

Case (c) can represent an imaging spectrometer camera where the detector array has a fill factor less than unity in the spectral direction, and thus gaps of insensitive area between detector elements. Depending on the degree of blur, the reduced fill factor can lead to an SRF peak width smaller than the sampling interval, as suggested in the figure, for any reasonable definition of peak width. The spectral sampling interval could still be taken as a reasonable definition of bandwidth for radiometric modeling, since this is the spectral bin defined by the spectrometer. The value of A^* from (35) will then account for the reduced response near band boundaries due to the fill factor.

Case (c) can also represent a hyperspectral camera based on a tunable filter, operated with a spectral sampling interval larger than the SRF peak width. For such cameras, the sampling interval is usually freely selectable by the user. It could then seem appropriate to define bandwidth as the width of the peak. A narrow SRF peak will then tend to give a large value of A^* in accordance with (35). However, if the spectral sampling interval is much larger than the peak width, this A^* value would seem unreasonable, since it does not account for the resulting undersampling of the spectral dimension. If instead the bandwidth is taken to be the sampling interval, the value of A^* will reflect the gaps in the spectral sampling.

Case (d) represents a camera where bands are overlapping, as illustrated by the notional square response shapes. Then, the sum of $A^*(\lambda)$ over all bands can become arbitrarily large, in principle, due to overlapping contributions from other bands. This is apparently inconsistent with the fundamental fact that measurement of photons is a destructive process. However, such a situation can arise for a camera based on tunable filters, not because photons are being measured multiple times, but because the bands are measured sequentially in time. Thus in such a case, if the bandwidth is taken to be the SRF peak width, values of A_j^* will give a fair indication of the light collection capability of the camera, as long as the user understands that bands are recorded sequentially in time.

The overall takeaway from the preceding examples is that for A^* values to be comparable across hyperspectral cameras based on a range of different technologies, the bandwidth cannot be defined as either the SRF peak width or the spectral sampling interval. In the current P4001 draft, a pragmatic definition is adopted as follows: For the purpose of defining A^*, the bandwidth is taken as the maximum of the SRF peak width and the spectral sampling interval. The exact definition of SRF peak width to be used in P4001 is under discussion, aiming to be robust over a range of different peak shapes. A camera specification according to the P4001 standard will then contain values for A^* which are directly comparable between cameras by being fairly well compensated for the effect on light collection that results from differences in bandwidth and spectral sampling.

C. Defining an Overall A^* for a Hyperspectral Camera

The overall value of A_{std}^* for light collection in a broadband or multispectral camera under a given illuminant, derived in Section V-D, is usable as a figure of merit for a hyperspectral camera as well. Starting from the detailed SRF shapes, the previous expression (33) can be directly applied. The need for a detailed SRF to determine A_{std}^* for a hyperspectral camera may seem contrary to the motivation of a per-band A_j^*. However, when preparing a camera specification according to the P4001 standard, the detailed SRF will be needed in any case, for determination of characteristics for spectral resolution and coregistration. If needed, (33) can be approximated using the set of per-band A_j^* and bandwidth:

$$A_{\mathrm{std}}^* = \frac{1}{L_{q,\mathrm{std}}} \int_\lambda \sum_j A_j^*(\lambda) L_{\lambda q,\mathrm{std}}(\lambda) \mathrm{d}\lambda \approx \frac{\sum_j A_j^* \Delta\lambda_j L_{\lambda q,\mathrm{std}}(\lambda_j)}{\sum_j \Delta\lambda_j L_{\lambda q,\mathrm{std}}(\lambda_j)}. \quad (36)$$

The reference to a particular illuminant tends to give more weight to bands with more signal in the expression for the overall A^*_{std}. In some cases, this may be inappropriate as a figure of merit for a hyperspectral camera, for example in applications where the camera is intended for measurement of reflectance (as opposed to radiance). The definition of an overall value of A^* can be decoupled from the illuminant spectrum by assuming a photon spectral radiance which is constant over all bands in (36). The expression then simplifies to

$$A^*_{\text{avg}} = \frac{\sum_j A^*_j \Delta\lambda_j}{\sum_j \Delta\lambda_j}. \tag{37}$$

This can be interpreted as an average value of A^* over the spectral range of the camera, which still accounts for differences in bandwidth.

VII. A^* for Cameras With Resampled Output Data

It is challenging to design optics with low distortion, not least in the case of hyperspectral cameras, where "smile" and "keystone" distortions are well known issues [17], [18]. At the same time, modern image sensors offer an abundance of small pixels. It is therefore increasingly attractive to resample the raw image data to correct for distortions in the camera optics. Resampling will complicate the model of signal and noise, and thus also the specification of camera performance. In the following, it is shown that A^* can be used as a comparative characteristic for light collection even for cameras employing resampling and binning schemes, under reasonable assumptions.

A. Resampled Signal Value

Hyperspectral image data may be resampled in the spectral or spatial dimensions, or both. The raw signal from the detector pixels on the image sensor is represented as a set of photoelectron counts $N_{e,k}$ where k is the index of such raw samples contributing to the output resampled value. The resampling operation is assumed to be a linear combination of these raw data samples with resampling coefficients a_{ijk} for pixel i and band j producing an output value

$$N_{r,ij} = \sum_k a_{\text{ijk}} N_{e,k}. \tag{38}$$

This is a resampled photoelectron count with physical dimension $[N_{r,ij}]$ = electrons. This representation of the signal is useful for the analysis here, even if this value is not an explicit stage in the camera signal chain, since $N_{r,ij}$ is proportional to the actual values in the output image (radiance, reflectance, DN, etc., depending on the scaling applied by the camera). The formalism in (38) does not assume a particular type of camera architecture, but can describe several different operations on the data, such as binning, smoothing, interpolation, or reshaping of response functions.

For radiometric characterization, it is assumed as before that the camera is viewing a spatially uniform, broadband calibration source. The spectrum is assumed to be smooth, with a small relative variation over the range of any spectral resampling. It is also assumed that the camera properties, such as sharpness and étendue, are smoothly and moderately varying in the resampling region. In the limit of a uniform, spectrally flat source, and uniform camera properties, the raw data values $N_{e,k}$ will tend to be equal. It will therefore be assumed here that the raw data values exhibit only moderate deviation from their mean $\langle N_{e,k}\rangle$

$$N_{e,k} \approx \langle N_{e,k}\rangle. \tag{39}$$

Consider first the simple case of binning. Then, raw data points are added together by setting some of the coefficients a_{ijk} to 1 and the remainder to zero. The resulting addition of raw data values clearly leads to a system which is well represented by the normal signal model, but for a correspondingly larger detector area. For other resampling operations, the coefficients can have arbitrary values, including negative values, depending on the operation performed. Then the mean magnitude of the resampled data may or may not be changed. A *generalized binning factor* B_r can be defined for the relative increase in total signal level that may occur in a resampling operation

$$B_r = \sum_k a_{\text{ijk}}. \tag{40}$$

Then, with reference to (39), an approximate model for the output value is

$$N_{r,ij} \approx B_r \langle N_{e,k}\rangle. \tag{41}$$

B. Noise and SNR in the Resampled Data

The noise in the resampled signal can be estimated by summation of variances. In the photon noise limit, well above the noise floor, the Poisson-distributed raw values $N_{e,k}$ are also estimates of their variance. Using the assumption of small differences between the raw values, we have for the resampled signal

$$\begin{aligned}\text{Var}\big(N_{r,ij}\big) &= \sum_k \text{Var}\big(a_{ijk} N_{e,k}\big) \\ &= \sum_k a^2_{\text{ijk}} \text{Var}\big(N_{e,k}\big) \approx \langle N_{e,k}\rangle \sum_k a^2_{\text{ijk}}.\end{aligned} \tag{42}$$

In the low-signal limit, the photon noise level $(\langle N_{e,k}\rangle)^{1/2}$ is less than the detector noise σ_{det} (dark current noise and readout noise). In a case where all contributing raw data samples are dominated by detector noise, we similarly find

$$\text{Var}\big(N_{r,ij}\big) \approx \sum_k a^2_{\text{ijk}} \sigma^2_{\text{det}} = \sigma^2_{\text{det}} \sum_k a^2_{\text{ijk}}. \tag{43}$$

Thus, in both limiting cases, the effect of the resampling operation on noise can be represented by a *noise degradation factor* D_r defined as

$$D^2_r = \sum_k a^2_{\text{ijk}}. \tag{44}$$

The total noise amplitude can then be approximated as

$$\text{SD}\big(N_{r,ij}\big) \approx D_r \sqrt{\langle N_{e,k}\rangle + \sigma^2_{\text{det}}}. \tag{45}$$

Note that thanks to the square-root dependence of noise on signal level, a given relative change in signal leads to approximately half as large relative change in noise, making the approximation in (45) less sensitive to deviations from the assumption of equal raw signals.

The signal-to-noise ratio after resampling will be

$$\mathrm{SNR}_r = \frac{N_{r,ij}}{\mathrm{SD}\left(N_{r,ij}\right)} \approx \frac{B_r}{D_r}\frac{\langle N_{e,k}\rangle}{\sqrt{\langle N_{e,k}\rangle + \sigma_{det}^2}} = \frac{\left(\frac{B_r}{D_r}\right)^2\langle N_{e,k}\rangle}{\sqrt{\left(\frac{B_r}{D_r}\right)^2\langle N_{e,k}\rangle + \left(\frac{B_r}{D_r}\right)^2\sigma_{\mathrm{det}}^2}}. \quad (46)$$

Comparing to (4), note that the effect of resampling on SNR is equivalent to a change in net light collection by a factor $(B_r/D_r)^2$. Thus, importantly, A^* for a resampled camera can still be determined using the photon transfer technique without any change to the measurement procedure. However, the estimated N_e will then not correspond to the actual photoelectron count, but rather to an equivalent photoelectron count for which the signal-dependent SNR is equal to that of the actual camera. Thus, the same noise model can be applied for cameras with and without resampling. This leads to the useful conclusion that A^*derived from a photon transfer measurement is a figure of merit that allows meaningful comparison of light collection between "black box" cameras, regardless of whether the signal is directly sampled or resampled.

C. Example Cases of Resampling

The effective binning factor B_r and the noise degradation factor D_r depend on the resampling scheme. Some examples in 1-D illustrate different cases.

1) A $4\times$ binning would have resampling coefficients $[1, 1, 1, 1]$ and 0 otherwise, giving $B = 4$ and $D = 2$. From (46), SNR increases by a factor 2 as expected.
2) Resampling by linear interpolation to an output point centered between two raw data points would have coefficients $[0.5, 0.5]$ and 0 otherwise, giving $B = 1$ and $D = 1/(2)^{1/2}$, thus increasing SNR by a factor $(2)^{1/2}$ in accordance with (46). In the same linear interpolation scheme, an output point centered on a raw data point would have $B = 1$ and $D = 1$, thus no change in SNR.
3) An operation like sharpening or deconvolution will have both negative and positive coefficients. A simple sharpening kernel might have nonzero coefficients $[-1, 3, -1]$, giving $B = 1$ and $D = (11)^{1/2} \approx 3.3$. SNR is reduced by the latter factor, illustrating the possibility of significant noise amplification and SNR degradation in resampling.

The second example here illustrates how the effect on noise by a resampling scheme may vary irregularly through the dataset if the output data points do not follow the input sampling pattern. For specification purposes, it then becomes necessary to account for this variation, for example by specifying both average and worst case values for the resulting A^*. When A^* values are given as metadata for a resampling-based camera, it may in principle be necessary to specify different values for each pixel and band in the FOV of the camera, in order to estimate noise with optimal accuracy. The P4001 standard will need to specify guidelines for determination of A^* taking the possibility of resampling into account.

VIII. Discussion

Modeling of the signal from a camera is well-established textbook material, and it would therefore be reasonable to question the need for a new metric for light collection, with an arguably trivial definition, introduced here. However, in the course of the P4001 work, it has become apparent that there is no established way to quantify net light collection for a "black box" camera. For P4001, it is important to avoid unnecessary complication of the camera specification, which will consist of more than 40 items in order to describe the many aspects of performance for a hyperspectral camera. Equation (24) shows clearly how A^* can replace a number of conventional quantities in an overall performance specification for a camera. Also, A^* is a figure of merit which is directly comparable between hyperspectral cameras having different bandwidths, focal lengths, or pixel sizes. Not least, A^* can be given a simple physical interpretation, which is beneficial for P4001 whose readership may include nonspecialist camera users. The use of this quantity in P4001 for camera specification and image metadata therefore appears justified. This article has argued that A^* may also be useful in other contexts.

Radiance values are most commonly given in energy units. For calculations involving A^*, these will have to be scaled by the wavelength-dependent photon energy into photon radiance quantities. This may be seen as a complication. However, since image sensors are based on photon detectors, and since photon statistics tends to be a dominating noise contribution, the use of photon radiance brings clear benefits.

While $A^*(\lambda)$ is well defined for monochromatic light in (26), the per-band A_j^* for a hyperspectral camera in (35) relies on a particular definition of bandwidth $\Delta\lambda_j$. As discussed in Section VI-B, it is not generally possible to define a unique value for the bandwidth. Therefore, values of A_j^* in a P4001-compliant camera specification may have some degree of variability depending on the details of the method used to determine bandwidth from the SRF. Work is ongoing to define a robust metric for peak width in P4001, in order to minimize such variability. Different hyperspectral cameras will undoubtedly tend to exhibit relative differences in A_j^* which are large compared to the variability resulting from bandwidth determination. Thus, values of A_j^* will still be a useful metric for camera comparison. Observe that when A_j^* values are used as metadata, the corresponding bandwidths $\Delta\lambda_j$ will also be given, and the product of these quantities will be as accurate as the radiometric calibration of the camera. By comparing (15) and (34), it is clear that a radiometric coefficient is a less well suited figure of merit, because it incorporates the bandwidth, and therefore will tend to favor the camera with a larger bandwidth.

The overall A_{std}^* value defined in (33) is useful as a comparative figure of merit for light collection in cases where a particular illuminant can be defined as relevant for

the application. For a hyperspectral camera, the illuminant-independent average A^*_{avg} defined in (37) can also serve as a single figure of merit. However, an important caveat must be made for cameras recording multiple bands sequentially. In that case, overlap between bands can lead to artificially high values for the overall value. This could be avoided by using a radiometric coefficient incorporating integration time instead of A^*, but then many of the other benefits of A^* would be lost. An important consideration is that values of A^*_j for different bands will depend strongly on wavelength due to the properties of optics and detectors. Therefore, comparison of cameras based on A^*_j values represented as a graph over wavelength will be significantly more informative than A^*_{std} or A^*_{avg}.

The uncertainty in the recorded pixel spectra from a hyperspectral camera can easily be dominated by errors due to imperfect coregistration [15], [18]. These errors are in effect a crosstalk from scene contrasts into the recorded light levels, so that the effect of coregistration on signal integrity becomes strongly dependent on the scene. For the present purpose of modeling radiometric properties of a camera, it can be noted that coregistration errors have no effect on the recorded image data if the incoming light varies only slowly with angle and wavelength, so that it can be taken as constant over a region surrounding the pixel under consideration, and around a band of a hyperspectral camera. This will be the case for calibration measurements with typical radiometric calibration sources, which is an underlying assumption for much of the discussion here. A^* can therefore be determined independently of the degree of coregistration error.

Stray light is another nearly unavoidable imperfection in hyperspectral cameras, and will tend to distort the values of A^*. It is well known that radiometric calibration must take stray light into account, for example by using a limited-size calibration source to avoid flooding the FOV. Stray light is beyond the scope of this article, but will be covered by P4001.

For cameras employing resampling, the value of A^* may have an irregular variation depending on the local values of resampling coefficients, as discussed in Section VII. This complicates the use of A^* as a figure of merit, but average values over a range of pixels or bands is still meaningful. The P4001 camera specification is foreseen to include the average and the worst case value. When A^* is given as metadata for a resampled image, separate values may have to be given for each pixel in the camera FOV, in principle. However, since the main use of A^* from metadata is likely to be estimation of noise, some approximate representation of A^* values may be adequate, depending on the particulars of the camera and application.

If the resampling operation, in the sense of Section VII, includes sharpening or similar operations, this may not be detectable in the output data. Such operations essentially trade an increase in noise against improvement in image sharpness. It has been shown here that photon transfer characterization of such cameras will yield values of A^* which correspond to an equivalent camera without resampling, and reflect the increase in noise. This is beneficial for the "black box" approach to camera characterization, and holds as long as the resampling is linear, and the resampling coefficients are fixed.

If instead the camera employs some form of "noise reduction" processing, or similar nonlinear processing stages, a photon transfer measurement will not yield correct results, and A^* becomes unobservable for a "black box" camera. This is even more true for cameras where the image formation is based on some form of reconstruction based on assumptions or prior knowledge of the scene. In these cases, the reconstructed image, as well as its level of noise and uncertainty, will tend to depend strongly on the peculiarities of the reconstruction method. For this and other reasons, P4001 will not apply fully to these classes of cameras.

The definition of A^* is motivated by its relevance to the noise model of photon detectors. Some camera types have a different noise model, for example those based on the Fourier transform spectroscopy, or other transformations of the recorded data. In those cases, A^* will still be useful for SNR estimation in cases where photon noise dominates, but the noise model will be different from the direct-sampling model (1) assumed here. In cases where other noise sources dominate, A^* is arguably an even more important quantity, since the SNR will be proportional to the net light collection, not to its square root. In such cases, a separate specification of noise is needed to estimate SNR, however.

Finally, it can be noted that beyond cameras, it is possible that A^* can be a useful way to describe light collection in other types of instruments involving imaging optics, for example spectrometers and other optical sensing systems.

IX. Summary and Conclusion

Motivated by needs arising in the IEEE P4001 standard development, and based on a generalized model of light collection by a "black box" camera in Section III-A, a quantity for net light collection has been proposed here, denoted A^*. This single quantity accounts for the étendue ("$A\Omega$ product") of an imaging system, as well as losses in the optics and detector, as shown notionally in (24). A^* can be interpreted as the pixel area of an equivalent lossless camera with standardized image-side geometry, as discussed in Section IV-B. Basically, A^* is the ratio of the photoelectron generation rate to incoming photon radiance, expressed in (26) for the case of monochromatic light. Since Poisson-distributed "photon noise" tends to dominate over other noise sources in normal operation of modern cameras, A^* facilitates estimation of signal-dependent SNR. Therefore, A^* is of interest both for camera specification and for image metadata.

This article proposes ways to specify A^* for conventional (Section V) and hyperspectral (Section VI-A) cameras, both as a wavelength-dependent quantity [(26) or (35), respectively] and as weighted averages over the spectral range (Sections V-D and VI-C, respectively). The derivation initially considers the signal from a single photodetector element, but it is shown in Section VII that cameras outputting resampled image data can be represented with the same model, using an effective value of A^*. In keeping with the P4001 "black box" approach to camera characterization, A^* is measurable without reference

to camera internals, by using the "photon transfer" method outlined in Section II-C.

In conclusion, A^* is a conceptually simple and physically interpretable quantity for expressing net light collection by a camera, with potential to make camera specifications more informative. Also, A^* can be useful as part of image metadata, enabling estimation of signal-dependent noise from the image data. A^* is foreseen to be incorporated in the IEEE P4001 standard for hyperspectral imaging, and it may also have potential for a wider range of uses.

ACKNOWLEDGMENT

The author would like to thank E. Ientilucci, D. Conran, J. Gilchrist, D. Perry, C. Durell, G. M. Selnesaunet, P. Rippis, and I. Kåsen, as well as the P4001 group, for helpful feedback and fruitful discussions.

REFERENCES

[1] T. Skauli, "Feasibility of a standard for full specification of spectral imager performance," *Proc. SPIE*, vol. 10213, Apr. 2017, Art. no. 102130H.

[2] IEEE Standards Association Project 4001. (May 14, 2018). *Standard for Characterization and Calibration of Ultraviolet Through Shortwave Infrared (250 nm to 2500 nm) Hyperspectral Imaging Devices*. [Online]. Available: https://standards.ieee.org/ieee/4001/7314/

[3] M. T. Eismann, *Hyperspectral Remote Sensing*. Bellingham, WA, USA: SPIE Press, 2012.

[4] T. Skauli, "Characterizing the dynamic range of a hyperspectral camera," *Proc. SPIE*, vol. 11727, Apr. 2021, Art. no. 117270D.

[5] T. Skauli, "How good is your spectral sensor? Figures of merit for coregistration and radiometric quality for spectral imagers and spectrometers," in *Opt. Sensors Sens. Congr., OSA Tech. Dig.* Optica Publishing Group, 2020, Paper ATu4I.1.

[6] T. Skauli, "Specifying radiometric performance of hyperspectral and conventional cameras—A minimal set of independent characteristics," *Proc. SPIE*, vol. 11392, Apr. 2020, Art. no. 113920B.

[7] T. Skauli, "Sensor noise informed representation of hyperspectral data, with benefits for image storage and processing," *Opt. Exp.*, vol. 19, no. 14, p. 13031, 2011.

[8] *Photography—Digital Still Cameras—Determination of Exposure Index, ISO Speed Ratings, Standard Output Sensitivity, and Recommended Exposure Index*, document ISO 12232:2019.

[9] R. C. Jones, "Quantum efficiency of photoconductors," in *Proc. IRIS*, vol. 2, 1957, p. 9.

[10] *Standard for Characterization of Image Sensors and Cameras*, Standard 1288, EMVA Release 4.0 Linear, Jun. 16, 2021.

[11] (Mar. 2007). *ASTER User's Guide Part II, Level 1 Data Products (Ver.5.1)*. [Online]. Available: https://lpdaac.usgs.gov/documents/69/AST_L1_User_Guide_V3.pdf

[12] J. R. Janesick, *Photon Transfer*, Bellingham, WA, USA: SPIE Press, 2007.

[13] J. Jemec, F. Pernus, B. Likar, and M. Bürmen, "Three-dimensional point spread function measurements of imaging spectrometers," *J. Opt.*, vol. 19, no. 9, Sep. 2017, Art. no. 095002.

[14] J. F. Silny, "Resolution modeling of dispersive imaging spectrometers," *Opt. Eng.*, vol. 56, Aug. 2017, Art. no. 081813.

[15] T. Skauli, "An upper-bound metric for characterizing spectral and spatial coregistration errors in spectral imaging," *Opt. Exp.*, vol. 20, no. 2, p. 918, 2012.

[16] *Calibration, Characterization and Use of Array Spectroradiometers*, CIE Standard 233:2019.

[17] P. Mouroulis, "Spectral and spatial uniformity in pushbroom imaging spectrometers," *Proc. SPIE*, vol. 3753, pp. 133–141, Oct. 1999.

[18] R. O. Green, "Spectral calibration requirement for Earth-looking imaging spectrometers in the solar-reflected spectrum," *Appl. Opt.*, vol. 37, no. 4, pp. 683–690, 1998.

[19] S. Beirle, J. Lampel, C. Lerot, H. Sihler, and T. Wagner, "Parameterizing the instrumental spectral response function and its changes by a super-Gaussian and its derivatives," *Atmos. Meas. Techn.*, vol. 10, no. 2, pp. 581–598, Feb. 2017.

Torbjørn Skauli (Member, IEEE) received the Ph.D. degree in physics from the University of Oslo, Oslo, Norway, in 1997.

He has worked since 1991 as a Scientist at the Norwegian Defence Research Establishment (FFI) at Kjeller, and since 2019 as a Professor at the University of Oslo, Department of Technology Systems, also at Kjeller. His research interests include optical imaging and remote sensing, including hyperspectral imaging and image sensor technology. He also engages in outreach, and currently heads a project sponsored by the Norwegian Research Council to adapt amateur radio as a tool for science education and recruitment.

Dr. Skauli is currently serving as the Vice Chair of the IEEE P4001 Standard Development Group.